ACTA MECHANICA SINICA, Vol.19, No.4, August 2003 ISSN 0567-7718
The Chinese Society of Theoretical and Applied Mechanics
Chinese Journal of Mechanics Press, Beijing, China
Allerton Press, INC., New York, U.S.A.

# LIFT FORCE ON ROTATING SPHERE AT LOW REYNOLDS NUMBERS AND HIGH ROTATIONAL SPEEDS*

YOU Changfu (由长福)† QI Haiying (祁海鹰) XU Xuchang (徐旭常)

(*State Key Lab of Clean Combustion of Coal, Tsinghua University, Beijing* 100084, *China*)

**ABSTRACT**: The lift force on an isolated rotating sphere in a uniform flow was investigated by means of a three-dimensional numerical simulation for low Reynolds numbers (based on the sphere diameter) ($Re < 68.4$) and high dimensionless rotational speeds ($\Gamma < 5$). The Navier-Stokes equations in Cartesian coordinate system were solved using a finite volume formulation based on SIMPLE procedure. The accuracy of the numerical simulation was tested through a comparison with available theoretical, numerical and experimental results at low Reynolds numbers, and it was found that they were in close agreement under the above mentioned ranges of the Reynolds number and rotational speed. From a detailed computation of the flow field around a rotational sphere in extended ranges of the Reynolds number and rotational speed, the results show that, with increasing the rotational speed or decreasing the Reynolds number, the lift coefficient increases. An empirical equation more accurate than those obtained by previous studies was obtained to describe both effects of the rotational speed and Reynolds number on the lift force on a sphere. It was found in calculations that the drag coefficient is not significantly affected by the rotation of the sphere. The ratio of the lift force to the drag force, both of which act on a sphere in a uniform flow at the same time, was investigated. For a small spherical particle such as one of about 100 $\mu$m in diameter, even if the rotational speed reaches about $10^6$ revolutions per minute, the lift force can be neglected as compared with the drag force.

**KEY WORDS**: lift force, drag force, numerical simulation, Magnus force, low Reynolds number

## 1 INTRODUCTION

The description of forces on a spherical particle could be considered to be the basis of a theoretical analysis in a gas-particle two-phase flow system. Generally, the rotation of particles takes place in many gas-particle cases and may be caused by a velocity gradient or a particle-particle collision or a particle-wall collision. The lift force developed due to the rotation of the particle as shown in Fig.1 is called the Magnus force in honor of its discoverer. Here, $F_{\mathrm{L}}$ is the lift force produced by the rotation of the sphere, $F_{\mathrm{D}}$ the drag force, $u_r$ the flow velocity, and $\omega$ the angular velocity. The Magnus force is caused by a pressure differential between the two sides of the particle resulting from the velocity differential due to the rotation. Magnus[1] and Newton [2] discussed the transverse force and gave an accepted explanation for its existence many years ago. Up to now, most of previous investigations on the lift force focused on a rotating cylinder. There were few studies concerning the lift force on a rotating sphere. Rubinow and Keller[3] obtained the lift force on a rotating sphere by using matched asymptotic expansions. In their analyses, the Reynolds number $Re(= \rho_f d u_r/\mu)$ was assumed to be much less than unity. Here $\rho_f$ is the fluid density, $d$ is the diameter of the sphere, $u_r$ is the relative fluid velocity between the sphere and the fluid flow, and $\mu$ is the fluid dynamics viscosity. Macoll[4],

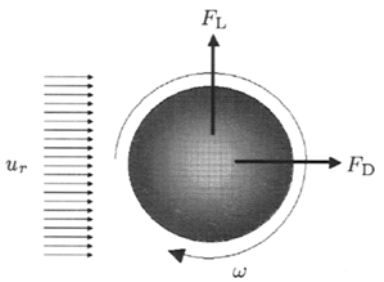


Fig.1 Lift force on a rotating sphere

Received 22 August 2002, revised 3 January 2003
* The project supported by the Special Funds for Major Basis Research Projects in China(G19990222)
† E-mail: youcf@te.tsinghua.edu.cn

Davies[5], Barkle and Auchterlonie[6] and Tanaka et al.[7] reported their experimental results of the lift force on a rotating sphere at Reynolds numbers exceeding $2 \times 10^3$. Tsuji et al.[8] obtained the lift force on a rotating sphere at Reynolds numbers from 550 to 1600 from trajectories of the sphere that impinged on an inclined plate and bounced.

For most application cases of the gas-particle two-phase flow, the Reynolds number based on the particle diameter often is limited in the range $Re < 100$. Such are the cases in the formation of the pulverized coal combustion, in the agglomeration of fine powders in gas flows, air filtration equipment, sewage disposal devices, fast fluidized beds, and so on. Most researches focused on the flow with higher Reynolds number, and their results cannot be used directly to solve the problem with a low Reynolds number. Recently, a few studies have been conducted for the lift force in the range of low Reynolds numbers. Oesterle and Bui Dinh[9] carried out the measurement of the lift force on a rotating sphere in a uniform flow using the trajectography technique at $10 < Re < 140$, and in the range of dimensionless rotational speed $\Gamma$ of between 1 and 6. Because of the difficulty in the experimental measurement, the measured values for the lift coefficient are not very accurate. Ben Salem and Oesterle[10] numerically investigated the influence of combined shear and rotation on the lift, drag and torque for the Reynolds number up to 20, and $-2 < \Gamma < +2$. The full Navier-Stokes equations in a spherical polar coordinate system were solved using a finite volume formulation based on a pressure correction procedure[11]. In their study, the lift and drag coefficients were found to be significantly sensitive to the grid parameters for a shear flow, so that reported results were restricted to the Reynolds number up to 20. Therefore, an expression of the lift force on the rotational sphere cannot be obtained from their results. Kurose and Komori[12] numerically studied the drag and lift forces acting on a rotating rigid sphere in a homogeneous linear shear flow by means of a three-dimensional numerical simulation. The effect of both the fluid shear and rotational speed of the sphere on the drag and lift forces were estimated in the range of the Reynolds number between 1 and 500, and of the dimensionless rotational speed of the sphere $\Gamma < 0.25$. An approximate expressions for the lift force coefficient were proposed for $Re < 500$, $\Gamma < 0.25$. Because of the lack of the wide validation for this expression, its accuracy remained a question.

With regard to the investigations on the lift force published in literatures, we think that what was said in Crowe et al.[13] for the lift force is still correct at the present time: "the lift coefficient due to rotation in regions of interest to fluid-particle flows ($1 < Re < 10^3$) is still an open question".

In order to accurately express the lift force for low Reynolds numbers, we present a numerical study of the flow over a rotating sphere in the range of $Re < 100$ and $\Gamma < 5$. The computational results are validated with the available data in literatures. Furthermore, an approximate expression for the lift coefficient against the rotational speed and Reynolds number is derived from the numerical results. Finally, in order to estimate the influence of the lift force on the particle movement, the ratio of the drag force to the lift force is discussed based on the computational results.

## 2 NUMERICAL SIMULATION

Using the numerical method, we study a flow with a uniform upstream over a rotating sphere in the range of $Re < 100$. The flow can be described by Navier-Stokes equations as follows

$$\nabla \boldsymbol{U} = 0 \tag{1}$$

$$\nabla(\rho \boldsymbol{U}\boldsymbol{U}) = -\nabla p + \mu \nabla^2 \boldsymbol{U} \tag{2}$$

where $\boldsymbol{U}$ and $p$ represent the fluid velocity and pressure, respectively. In the present study, external body forces such as gravitation are ignored.

In the present numerical study of the lift force on a rigid sphere, the computational domain is schematically shown in Fig.2. The sphere diameter is 100 $\mu$m for all computational cases. Because of the symmetry of the flow field with regard to the $yz$-plane in the range of Reynolds numbers, only a half of the flow over the sphere is considered in the calculations. The sphere is rotating with a constant rotational speed around a transverse axis through the center of the sphere. The inlet velocity is in a uniform distribution,

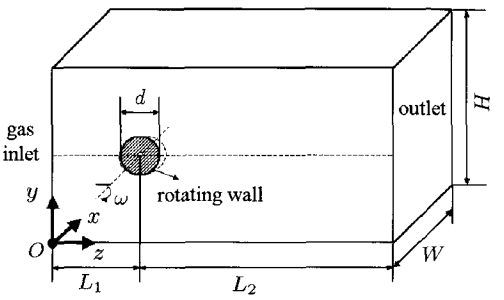


Fig.2 Coordinate system and computational domain

and the fully developed flow is taken as the outlet condition. Other faces are symmetrical boundaries. The discussion of the computational accuracy will be made in the next sections.

The present calculation employs a finite volume method for the spatial discretization of the governing equations. Most of the meshes are unstructured in the calculation, such as the tetrahedral mesh. Figure 3 displays the mesh distribution near the sphere. It can be seen that the mesh was designed to have a non-uniform distribution so that the mesh adjacent to the sphere has a very fine resolution and the size of the mesh increases as it moves away from the sphere. The size of the grid adjacent to the sphere surface is the smallest in the entire domain and is $5\,\mu$m; the maximum mesh size is $20\,\mu$m. The QUICK scheme with a three-order discretization accuracy is used to avoid the numerical diffusion and obtain an accurate flow field. The SIMPLE algorithm[14] is used to deal with the coupling between velocity and pressure, and the convergent criteria for the residue for all variables are set to be $10^{-06}$. A typical case simulation requires about 10 h CPU time on a PC with Pentium II-400 processor.

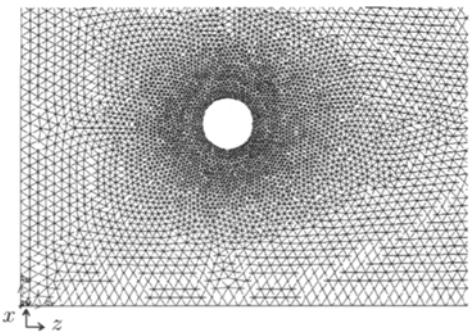


Fig.3 Mesh distribution near the sphere

The hydrodynamic force on a rotating sphere in a uniform flow is usually resolved into the drag force $F_{\rm D}$, in the direction of the relative motion, and the lift force $F_{\rm L}$, which is orthogonal to the direction of the relative motion. The drag and lift forces can be obtained by summing both of the pressure and viscosity forces in the $z$- and $y$-directions, respectively, and in a dimensional form, are defined by

$$F_{\rm D} = F_{{\rm D},p} + F_{{\rm D},f} = -\iint_S p\boldsymbol{e}_z \boldsymbol{n}{\rm d}S + \iint_S \boldsymbol{n}\boldsymbol{\tau}\boldsymbol{e}_z {\rm d}S \tag{3}$$

$$F_{\rm L} = F_{{\rm L},p} + F_{{\rm L},f} = -\iint_S p\boldsymbol{e}_y \boldsymbol{n}{\rm d}S + \iint_S \boldsymbol{n}\boldsymbol{\tau}\boldsymbol{e}_y {\rm d}S \tag{4}$$

where $\boldsymbol{n}$ is the outward-pointing unit normal vector at the particle surface, and $\boldsymbol{\tau}$ is the viscous stress tensor. These force components are characterized by the dimensionless coefficients $C_{\rm D}$ and $C_{\rm L}$, defined by

$$F_{\rm D} = C_{\rm D}\frac{1}{2}\rho_f u_r^2 S \tag{5}$$

$$F_{\rm L} = C_{\rm L}\frac{1}{2}\rho_f u_r^2 S \tag{6}$$

where $\rho_f$ is the fluid density, $u_r$ the relative velocity between the flow and sphere and $S$ the projected sectional area of the sphere. The rotational speed of the sphere is usually represented by a ratio of the equatorial velocity of the sphere to the sphere-fluid relative velocity, which is defined as

$$\Gamma = \frac{{\rm d}\omega}{2u_r} \tag{7}$$

where $\omega$ is the angular velocity of the sphere of diameter $d$.

The Reynolds number based on the sphere diameter is

$$R_e = \frac{\rho_f {\rm d}u_r}{\mu} \tag{8}$$

With the selected sphere diameter, $d = 100\,\mu$m, the Reynolds number of from 0.5 up to 68.4 can be obtained by varying the relative velocity $u_r$ between 0.073 m/s and 10 m/s.

According to the studies on the lift force on a sphere in literature, the size of the computational domain strongly affects the accuracy of calculation. Table 1 gives some sizes used by other studies and by the present study. Here $r_{\rm min}$ is the minimum distance between the center of the sphere and the outer boundary location, and $r_{\rm sphere}$ is the radius of the sphere. Two tests are carried out to examine the sensitivity of the solution to the position of the outer boundary. Using the same values of the Reynolds number $Re = 68.4$ and of the rotational speed $\Gamma = 5$, and a similar mesh size, we computed for both small and large domain sizes: $(L1, L2, W, H) = (4d, 12d, 3.5d, 7d)$ and $(10d, 20d, 10d, 20d)$. In Table 2, the values of the drag and lift forces obtained from the large and small domain simulations are compared. It can be seen that the values of the drag and lift forces obtained by the small domain simulations are larger than those obtained by the corresponding simulations using the larger domain. There are small discrepancies due to the truncation of the domain. Because the number of mesh is considerable for the large domain simulation, the computational requirements (the number of floating point operations and the memory requirements) are very large. Hence, we could not conduct simulations with larger domains, the values of $(L1, L2, W, H) = (4d, 12d, 3.5d, 7d)$ are used in all subsequent calculations.

**Table 1 Selections of the computational domain by some researchers**

| | |
|---|---|
| Dandy and Dwyer [15] | |
| for linear shear flow, $0.1 \leq Re \leq 100, \Gamma = 0.0$ | $r_{\min} = 12.5d = 25r_{\text{sphere}}$ |
| Ben Salem and Oesterle [10] | $r_{\min} = 55d = 110r_{\text{sphere}}$ |
| for linear shear flow, $Re \leq 20, \Gamma < 2$ | (for very small $Re$) |
| Cherukat et al.[16] | |
| for linear shear flow, $Re \sim O(1), \Gamma = 0.0$ | $r_{\min} = 37.5d = 75r_{\text{sphere}}$ |
| Kurose and Komori[12] | |
| for linear shear flow, $1 \leq Re \leq 500, \Gamma < 0.25$ | $r_{\min} = 5d = 10r_{\text{sphere}}$ |
| Lee and Wilczak[17] | |
| for linear shear flow, $20 \leq Re \leq 500, \Gamma = 0.0$ | $r_{\min} = 6d = 12r_{\text{sphere}}$ |
| Present study | $r_{\min} = 3.5d = 7r_{\text{sphere}}$ |
| for uniform flow, $Re \leq 68.4, \Gamma < 5$ | $(L1 = 4d, L2 = 12d, W = 3.5d, H = 7d)$ |

**Table 2 Comparison between the results obtained with small and large computational domains**

| $(L1, L2, W, H)$ | $C_{\text{D}}$ | $C_{\text{L}}$ |
|---|---|---|
| $(4d, 12d, 3.5d, 7d)$ | 1.42 | 1.61 |
| $(10d, 20d, 10d, 20d)$ | 1.3 | 1.5 |

## 3 RESULTS AND DISCUSSIONS

### 3.1 Accuracy of the Numerical Simulation

In order to test the accuracy, calculations were made for two different cases: flows over a stationary sphere at $Re < 100$ and over a rotating sphere at $Re < 1$.

Figure 4 shows the comparison of the drag force on a stationary sphere obtained by present simulation with that reported by Schlichting[18]. It is noted that the agreement is reasonable at low Reynolds numbers. But it also can be seen that the discrepancy increases for higher Reynolds numbers. This may be due to the numerical diffusion in the calculation. Because the mesh type selected in the present study is tetrahedral, the flow can never be aligned with the grid. It is clear that, at higher Reynolds numbers, the flow behind the sphere becomes more complex. With increasing the Reynolds number, the wake size and separation angle increase. As a consequence, the numerical diffusion becomes more noticeable, which affects the computational accuracy.

Another validation is the calculation of the lift force on a rotating sphere for the Reynolds number $Re = 0.5$, with a comparison with the theoretical results of Rubinow and Keller[3]. The theoretical solution of Rubinow and Keller was expressed by

$$C_{\text{L}} = 2\Gamma \tag{9}$$

Values of some parameters used in the present calculations are given in Table 3. Figure 5 shows a comparison between the predicted lift coefficient and the values calculated using Eq.(9) in the range of $Re < 1$. It can be seen that a very good agreement can be achieved.

**Table 3 Computational conditions for testing the numerical simulation**

| | |
|---|---|
| $u_r/(\text{m}\cdot\text{s}^{-1})$ | 0.073 |
| $\mu/(\text{kg}\cdot(\text{m}\cdot\text{s})^{-1})$ | $1.789\,4\times10^{-5}$ |
| $\rho_f/(\text{kg}\cdot\text{m}^{-3})$ | 1.224 |
| $d/\mu\text{m}$ | 100 |
| $Re$ | 0.5 |
| $\Gamma$ | 0.1,0.2,1.0,4.0 |
| $\omega/(\text{rad}\cdot\text{s}^{-1})$ | 146,292,1 460,5 480 |

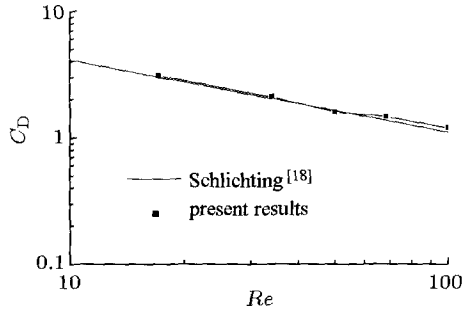


Fig.4 Effects of Reynolds number on drag coefficient on a particle

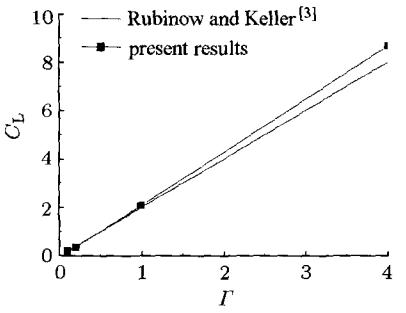


Fig.5 Comparison between theoretical and computational results for $Re = 0.5$

Because most calculations in the present study are for $Re > 1$, the accuracy at such Reynolds numbers should be paid more attentions. According to the results reported by Ben Salem and Oesterle[10], at a very small Reynolds number, a very large size of the computational domain is required to obtain accurate results, however, at a higher Reynolds number, this value may be reduced without loss of accuracy. Thus it can be seen that the size chosen in the present calculation in the range of higher Reynolds numbers is enough to provide reliable results regarding the hydrodynamic forces and flow patterns.

### 3.2 Effect of Reynolds Number $Re$ and Rotational Speed $\Gamma$ on Lift Coefficient $C_L$

In order to determine the relation of the lift coefficient against the Reynolds number and the rotational speed, the detailed numerical simulations of the lift force on a rotating sphere in a uniform flow are carried out in the range of $Re \leq 68.4$ and $\Gamma \leq 5$.

Figure 6 shows the lift coefficients of the rotating sphere at different Reynolds numbers. With increasing $\Gamma$ or decreasing Reynolds number, the increasing trend for the lift coefficient is obviously observed. Moreover, the results seem to indicate that the lift coefficient decreases very slightly with increasing $Re$ at a fixed value of $\Gamma$, and the influence of $\Gamma$ gradually vanishes at higher Reynolds numbers. Similar results were obtained in the experimental study of Oesterle and Bui Dinh[9]. Figure 7 gives a comparison between the present and Oesterle and Bui Dinh's results. In Oesterle and Bui Dinh's experiments, the data were much scattered. It is found from the rough comparison, the magnitude of the lift coefficient obtained by the present numerical simulation is in a quantitative agreement with that obtained experimentally. Fitting the numerical results using the least square method,

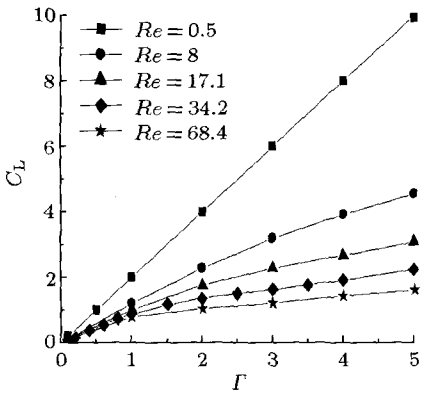


Fig.6 The computational values of the lift coefficient as a function of the rotational speed at different Reynolds numbers

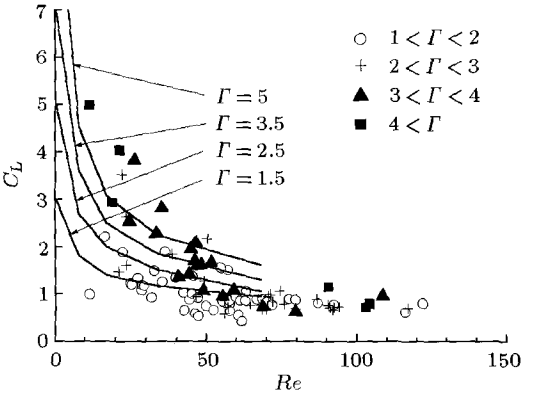


Fig.7 The computed lift coefficient as a function of the Reynolds number $Re$. Present results (solid line) are compared to the experimental results by Oesterle and Bui Dinh[9] (symbols)

an empirical Eq.(10) is obtained to express the lift coefficient in terms of the Reynolds number and the rotational speed, $\Gamma$

$$\begin{aligned} C_{\mathrm{L}} &= A(1 - B^{\Gamma}) \\ A &= 1.51 + 5.69\exp(-Re/18.62) + \\ &\quad 26.32\exp(-Re/3.65) \\ B &= 0.56 + 0.37\exp\left(-\frac{Re - 0.5}{26.39}\right) \end{aligned} \tag{10}$$

Figure 8 shows the flow patterns at different rotational speeds in the $yz$-plane. As the no-slip boundary condition is used on the surface, the flow velocity near the sphere gradually increases with increasing the sphere rotational speed. When the sphere is rotated with a low spin speed, such as in the situation of $\Gamma = 0.1$, the wake can also be observed behind the sphere. With continually increasing the rotational speed, the tangential velocity of the fluid on the surface of the sphere gradually weakens the wake size until the wake behind the sphere is completely destroyed, as shown in Fig.8 when $\Gamma = 1.0, 3.0, 5.0$. Figure 9 shows the distribution of $z$-component velocity along a vertical centreline. For such a flow case, there is a large region beneath the particle where the flow is reversed with regards to the upstream flow. The distance between the bottom surface of the sphere and the turning point approaches the sphere diameter, 100 $\mu$m. If this particle is located in a multi-particle system, the spheres around it may be affected by the reversed flow. On the other hand, it can be observed that a considerable velocity gradient appears near the sphere due to a considerable high rotational speed. For such a flow, there is some doubt as to

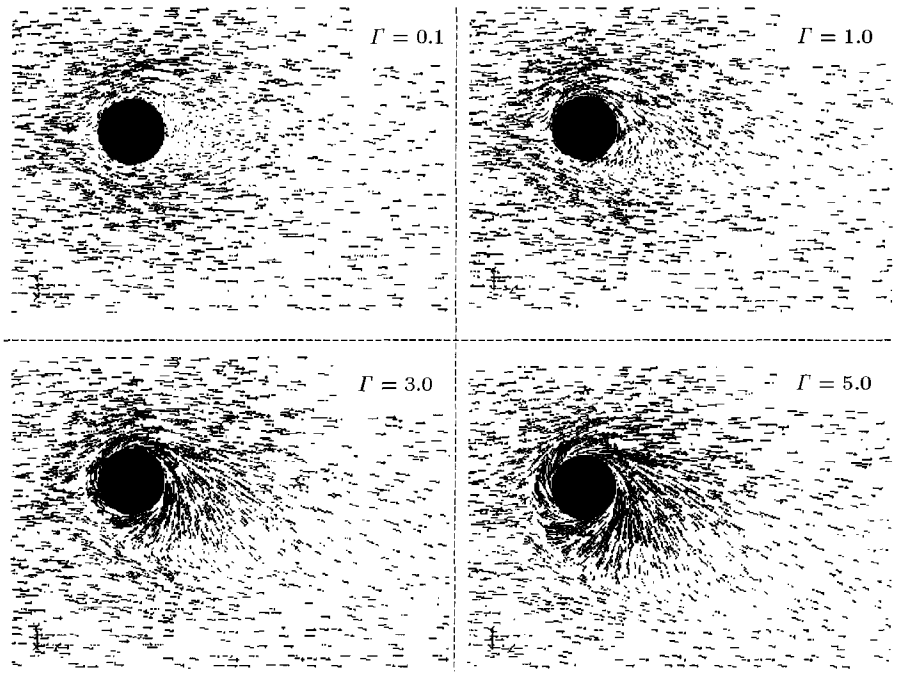


Fig.8 The flow patterns at different spin parameters $\Gamma$ at $Re = 34.2$
(In order to avoid the vector arrows' lap over, only parts of velocities are shown)

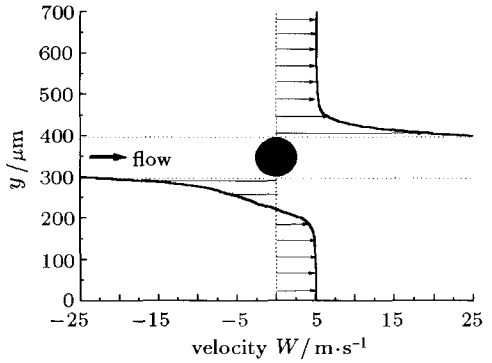


Fig.9 The velocity distribution in a vertical centreline at $Re = 34.2$ and $\Gamma = 5$

whether the Navier-Stokes equations can be reasonably used. The further investigations on the flow over a sphere with a high rotational speed are required.

The lift force on a rotating sphere is equal to the sum of the pressure and viscous force in the vertical direction. Figure 10 gives the ratio of the pressure $C_{L,p}$ to the viscous force $C_{L,f}$ as a function of the rotational speed and the Reynolds number. It can be seen that the pressure $C_{L,p}$ contributes greatly to the total lift $C_L$ as compared with the viscous force $C_{L,f}$. With increasing the rotational speed of the sphere, the ratio of $C_{L,p}$ to $C_{L,f}$ rapidly decreases. However, for higher Reynolds numbers, with increasing the rotational speed, this ratio seems tend to increase, as shown in the figure that, at $Re = 68.4$, the ratio at $\Gamma = 5$ is larger than that at $\Gamma = 3$. For a fixed rotational speed, with increasing the Reynolds number, the ratio $C_{L,p}$ to $C_{L,f}$ increases. A similar trend has also been found by Kurose and Komori[12], who carried out the calculation of the lift force on a rotating sphere in a uniform flow for $\Gamma < 0.25$ and a large Reynolds number range of from 1 to 500. Figure 11 shows the comparison between the present results at $\Gamma = 0.1$ and Kurose and Komori's results at $\Gamma = 0.16$. The qualitative agreement can be found between them, whereas there exists an obvious quantitative difference. The comparison of the present lift force expression (10) with that obtained by Kurose and Komori[12] (expression (3.11) in their paper) is shown in Fig.12 for $Re$ near unity. It shows a large difference between them, and the present result is close to the Rubinow and Keller's results obtained theoretically for small values of the Reynolds number. To

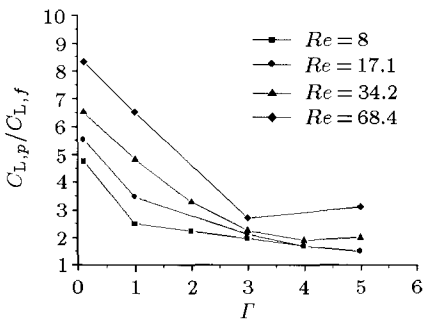


Fig.10 Ratio of contribution of pressure $C_{L,p}$ to that of viscous force $C_{L,f}$ in the total lift coefficient $C_L$

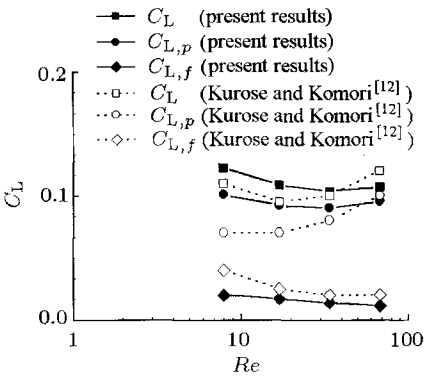


Fig.11 Comparisons of lift coefficients $C_L$, $C_{L,p}$, $C_{L,f}$ for a rotating sphere between the present results for $\Gamma = 0.1$ and that by Kurose and Komori[12] for $\Gamma = 0.16$

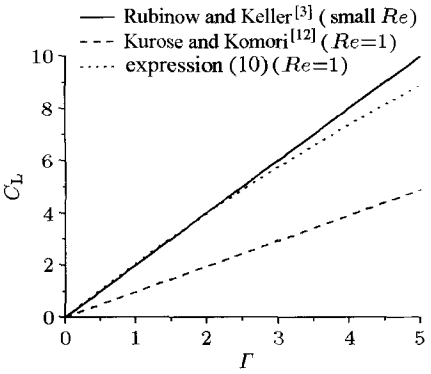


Fig.12 Comparisons of the expression (10) with the Kurose and Komori's result at $Re = 1$

the best of our knowledge, the sudden flow change would not happen from $Re = 0.5$, where the computation had been validated in section 3.1, to $Re$ near unity. Therefore, the value of the lift coefficient at $Re = 1$ should be near that predicted by Rubinow and Keller's equation (9) for $Re$ less than unity. It means that the present relationship (10) is more accurate than that obtained by Kurose and Komori.

### 3.3 Effect of Rotation on Drag Force

In the previous studies[10,12], the drag coefficient $C_D$ was found not significantly influenced by the rotation of the sphere. In the present calculation of the drag force at low Reynolds numbers, similar results are also obtained. Figure 13 gives the computational results of $C_D$ at low Reynolds numbers. With increasing the rotational speed for a fixed value of the Reynolds number, the drag coefficient varies slightly. However, with continuously increasing the rotational speed such as more than $\Gamma = 5$, $C_D$ tends to decrease for all of Reynolds numbers used in the calculation.

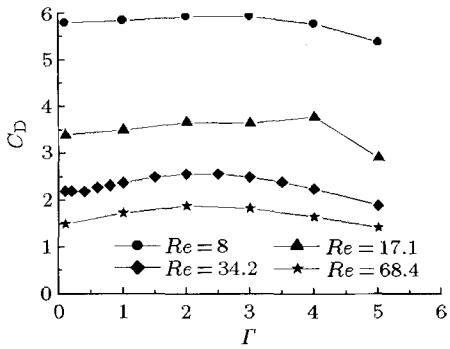


Fig.13 The drag coefficient as a function of rotational speed at different Reynolds numbers

### 3.4 Ratio of Lift Force to Drag Force

In theoretical analyses and numerical simulations of the gas-particle two-phase flow, the ratio of the lift force to the drag force is of interest. Sometimes, the lift force produced by the particle rotation was neglected as compared with the corresponding drag force on it. Because of lack of knowledge about the lift force in the range of low Reynolds numbers, this neglect of the lift force on a particle was not justified. On the other hand, because of the lack of the relationship expressing the lift coefficient in terms of the Reynolds number and rotational speed in the corresponding range of the Reynolds number to the practical case, the numerical simulations of the particle motion can not be conducted using a relationship of previous results, such as Rubinow and Keller's equation (9). If the practical Reynolds number is not in the range, where the lift relationship was obtained, the calculation of the lift force will not be correct.

Figure 14 gives the ratio of the lift coefficient to the drag coefficient at low Reynolds numbers. With the increase of the rotational speed, this ratio rapidly increases. Also, it can be seen that the data do not have a very large scatter with the variation of the Reynolds numbers. To estimate the value of the lift force on a rotating sphere at low Reynolds numbers,

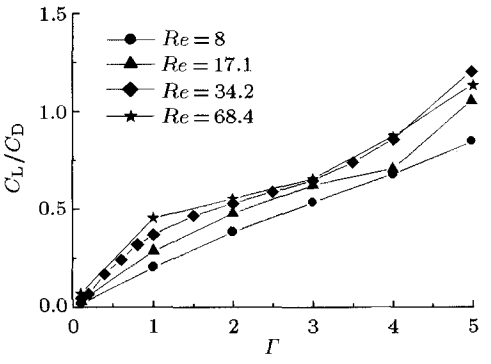


Fig.14 The ratio of $C_L$ to $C_D$ as a function of $\Gamma$ at different Reynolds numbers

an empirical equation is obtained by fitting data shown in Fig.14.

$$C_L/C_D = 0.438\,84\Gamma - 0.124\,71\Gamma^2 + 0.015\,89\Gamma^3 \quad (11)$$

The results of the present study may be of interest for the case of the particle motion in a pulverized coal boiler or in a reactor of flue gas desulfurization. The particle diameter is typically of order of 100 $\mu$m in these cases. When the dimensionless rotational speed $\Gamma$ approaches about 5, i.e., when the rotational speed is about 4 800 000 rpm, the value of the lift force on the sphere is close to that of the drag force. Generally, it is rarely the case for the sphere to come up with such a considerable rotational speed. Shi et al.[19] measured the rotational speed of a fine particle fired in a practical industrial pulverized coal boiler by using the multi-pulse laser holography. When a particle came into collision with the wall surface, the rotational speed approached only about 1800 cycle per second (108 000 rpm). When a spherical particle moves with that rotational speed, and the Reynolds number also falls into the range less than 68.4, the corresponding lift-to-drag ratio can be estimated to be equal to about 0.01. Therefore, it is reasonable neglecting the lift force in the theoretical analyses, numerical simulations as well as experimental measurements of a two-phase flow.

## 4 CONCLUSIONS

In the present study, the numerical simulations of the flow over a rotating sphere in a uniform flow are carried out at low Reynolds numbers. The conclusions can be drawn as follows:

(1) The lift force on a rotating sphere in a uniform flow is successfully investigated by using numerical simulation in the range of the Reynolds number $Re \leq 68.4$ and of the dimensionless rotational speed $\Gamma \leq 5$. Through comparing the computational results with the theoretical data, the accuracy of the simulation is tested, and a reasonable agreement is obtained.

(2) A relationship expressing the lift coefficient in terms of the Reynolds number and rotational speed is obtained, which is more accurate than those obtained by previous studies.

(3) The drag force is slightly influenced by the sphere rotation in the range of $Re \leq 68.4$ and $0 \leq \Gamma \leq 5$, and its variation with the increasing rotational speed mainly depends upon that of the pressure value on the sphere surface.

(4) The ratio of the lift force to the drag force, both of which act on a rotating sphere in a uniform flow at the same time, is investigated. For a small particle such as one of about 100 $\mu$m in diameter, even when the rotational speed approaches about 100 000 rpm, the lift force can be neglected as compared with the corresponding drag force.

## REFERENCES


1 Magnus G. Uber die Abweichung der Geschloss, und eine auffallende Erscheinung bei rotierenden Korpern. *Poggendorfs Annalen der Physik und Chemic*, 1853, 88: 1

2 Newton I. *Phil Trans Roy Soc*, 1672, 7: 3078

3 Rubinow SI, Keller JB. The transverse force on a spinning sphere moving in a viscous fluid. *J Fluid Mechanics*, 1961, 11: 447~459

4 Macoll JH. Aerodynamics of a spinning sphere. *J Roy Aero Soc*, 1928, 32: 777~798

5 Davies JM. The aerodynamics of golf balls. *J Appl Phys*, 1949, 20(9): 821~828

6 Barkle HM, Auchterlonie LJ. The Magnus or robins effect on rotating spheres. *J Fluid Mechanics*, 1971, 47, part3: 437~448

7 Tanaka T, Yamagata K, Tsuji Y. Experiment of fluid forces on a rotating sphere and spheroid. In: KSME ed. Proc. Second KSME-JSME Fluids Eng Conf, Seoul 1990. Seoul: KSME Press, 1990. 366~369

8 Tsuji Y, Morikawa Y, Mizuno O. Experimental measurement of the Magnus force on a rotating sphere at low Reynolds numbers. *J Fluid Engineering*, 1985, 107: 484~488

9 Oesterle B, Bui Dinh T. Experiments on the lift of a spinning sphere in a range of intermediate Reynolds numbers. *Experiments in Fluids*, 1998, 25: 16~22

10 Ben Salem M, Oesterle BA. Shear flow around a spinning sphere: numerical study at moderate Reynolds numbers. *Int J Multiphase Flow*, 1998, 24(4): 563~585

11 Van Doormaal JP, Raithby GD. An evaluation of the segregated approach for predicting incompressible fluid flows. In: ASME ed. Proc '85 ASME Heat Transfer Conference, Denver, 1985, Denver: ASME Press, 1985, Paper 85-HT-9

12 Kurose R, Komori S. Drag and lift forces on a rotating sphere in a linear shear flow. *J Fluid Mechanics*, 1999, 384: 183~206

13 Crowe C, Sommerfeld M, Tsuji Y. Multiphase Flows with Droplets and Particles. USA: CRC Press, 1998

14 Patankar SV. Numerical Heat Transfer and Fluid Flow. Washington DC: Hemisphere, 1980

15 Dandy DS, Dwyer H. A sphere in shear flow at finite Reynolds number: effect of shear on particle lift, drag, and heat transfer. *J Fluid Mechanics*, 1990, 216: 381~410

16 Cherukat P, McLaughlin JB, Dandy DS. Computational study of the inertial lift on a sphere in a linear shear flow field. *Int J Multiphase Flow*, 1999, 25(1): 15~33

17 Lee S, Wilczak JM. The effects of shear flow on the unsteady wakes behind a sphere at moderate Reynolds numbers. *Fluid Dynamics Research*, 2000, 27(1): 1~22

18 Schlichting H. Boundary Layer Theory. New York: McGraw-Hill, 1979

19 Shi XG, Xu XC, Feng JK. The analysis of forces on particle moving in turbulent flow. *Chinese Journal of Engineering Thermophysics*, 1989, 10(3): 320~325